Validation of cathare code on the 3d rosa-lstf pressure vessel

S. Carnevali, P. Bazin

VALIDATION OF CATHARE CODE ON THE 3D ROSA-LSTF PRESSURE VESSEL

S.Carnevali , P. Bazin
CEA/DEN/DM2S/STMF/LMES, 91400 Gif-sur-Yvette, France
sofia.carnevali@cea.fr

ABSTRACT

The Commisariat à l'Energie Atomique et aux Energie Alternatives (CEA) is performing an important work aimed to validate the 3D modelling for the CATHARE code since the necessity to better simulate the 3D effects observed during nuclear accidents experimental tests. The attention is focused on the reactor vessel behaviour. This paper presents a first validation of the code on the Japanese ROSA-LSTF installation for the test 1 of the OECD/NEA ROSA2 project. An important effort is focused on the 3D modelling of the entire ROSA-LSTF pressure vessel by one single 3D module. A first validation is performed for this test 1 corresponding to an intermediate (17%) hot leg break. Starting from the previous ROSA integral system input deck, the 1D-0D components, generally employed to simulate the entire pressure vessel, are replaced by this single 3D CATHARE module. A very good agreement between calculated and experimental results is obtained and presented in this paper. Furthermore the comparison with the previous 1D-0D results shows a better consistency of the 3D approach with experimental data. It stresses out the importance to better investigate the 3D phenomena and the necessity to carry on with the 3D validation. The non-homogenous temperature distribution at the core exit, the influence of the particular 3D geometry or the specific 3D flowrate direction and the presence of the CCFL phenomenon in the core support plate are dealt with in detail. As conclusion, a first validation of CATHARE 3D module is completed and a better understanding of 3D phenomena starting from the code results is shown possible, complementary to the experimental evidence.

KEYWORDS: CATHARE, ROSA-LSTF, 3D, validation, pressure vessel

I – INTRODUCTION

This paper deals with the 3D modelling of the pressure vessel of the ROSA-LSTF (Large Scale Test Facility) facility performed with CATHARE 2 V2.5_3 code. One single 3D model is foreseen for this purpose.

The LSTF, the so called ROSA (Ring OF Safety Assessment) facility, is located at the Tokai Research Establishment of the JAEA in Japan. It was used in the frame of the Japanese

ROSA-IV and ROSA-V program since 1985 to study thermo-hydraulics responses of LWRs during loss-of-coolant accidents. During the years, different versions of this facility are proposed to simulate specific situations. In this work the attention is focused on the particular version of the LSTF geometry emploied during the Japanese ROSA-V program and the OECD/NEA ROSA and ROSA2 project. Since today, the integral systems are modelled by several OD-1D elements. Purpose of this work is the substitution of a single 3D module into a 0D-1D integral system. Calculated and experimental results may be compared and the CATHARE code validated during different scenarios. The final goal of this analysis is so the validation of the 3D model in the CATHARE code.

II - ROSA FACILITY

The ROSA-LSTF test facility simulates the full-scale height and 1/48 volumetrically scaled-down representation of a Westinghouse four loops PWR with a thermal power of 3423 MW (see Figure 1). It is composed by two primary loops corresponding to the four-loops of a PWR: the intact loop A and the broken loop B. As shown in Figure 1, the pressurizer is connected to the hot leg A. The break nozzle and the break circuit are located on the loop B.

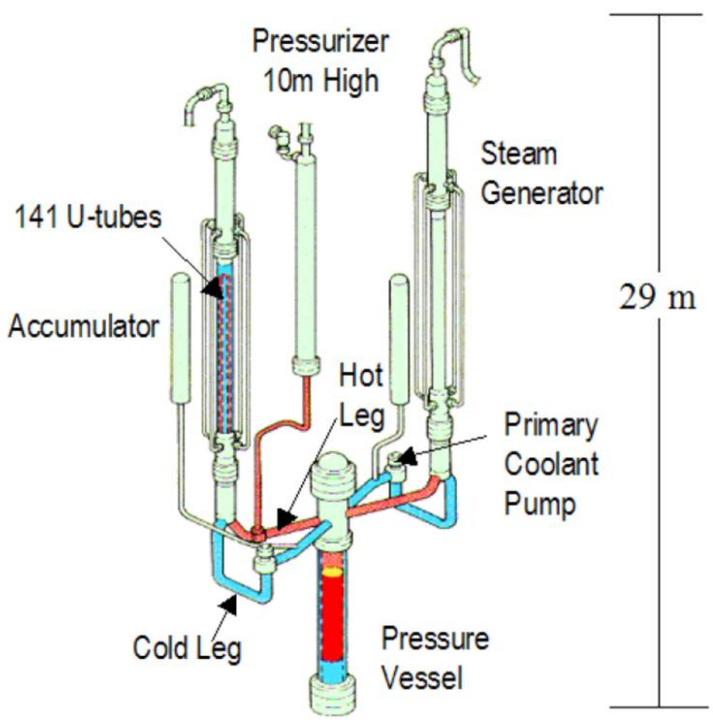

Figure 1. ROSA tests facility [1]

Table I shows the comparison between some principal PWR dimensions and the corresponding scaled LSTF.
The core bundle is composed of 1008 rods electrically heated. The dimensions of these rods (diameter, length, layout…) are those of a 17x17 assembly consistent with a rod bundle used in a PWR. The complete description of the experimental facility can be found in [1].

Table I. LSTF design data [1]

Items		LSTF	Reference PWR	LSTF/PWR
Number of SGs		2	4	1/2
Max. Heat Removal Rate*	(MW)	35.7	856	1/24
Number of U-tubes*		141	3382	1/24
Feedwater Flow Rate*	(kg/s)	2.76	469	1/170
Steam Flow Rate*	(kg/s)	2.76	468	1/170
Pressure in SG Steam Dome	(MPa)	7.34	6.13	1.20/1
Temperature in SG Steam Dome	(K)	562.2	550.2	1.02/1
Temperature at SG Inlet	(K)	598.1	598.1	1/1
Temperature at SG Outlet	(K)	562.4	562.4	1/1
Temperature Difference between SG Inlet and Outlet	(K)	35.7	35.7	1/1
Inner Diameter of U-tube	(mm)	19.6	19.6	1/1
Outer Diameter of U-tube	(mm)	25.4	22.23	1.14/1
Total Inner Surface Area of U-tubes*	(m^2)	171	4214	1/24.6
Total Outer Surface Area of U-tubes*	(m^2)	222	4780	1/21.5
Average Length of U-tubes	(m)	19.7	20.2	0.975/1
Wall Thickness of U-tube	(mm)	2.9	1.3	2.23/1
Pitch of U-tubes	(mm)	32.5	32.5	1/1

*Designed value per one SG.

II - 3D MODELLING

For the modelling of the pressure vessel, a particular discretisation into three different spatial zones is taken into account.

Axial discretisation
A first division is so realized along the vertical line (axial) as shown in Figure 2. Pressure vessel is about 10.9 m high and it is divided into 26 meshes of about 400 mm high. Each zone is characterised by meshes with the same porosity and the same hydraulic diameter (the so called 'zone'). The 26 meshes are fixed starting from the axial core discretisation to respect the axial power distribution [1]. Indeed the axial core power is described by a series of nine heat flux steps of about 400 mm high. Starting from this condition, meshes in the entire pressure vessel are automatically defined. Figure 2 well shows the axial discretisation proposed into CATHARE code.

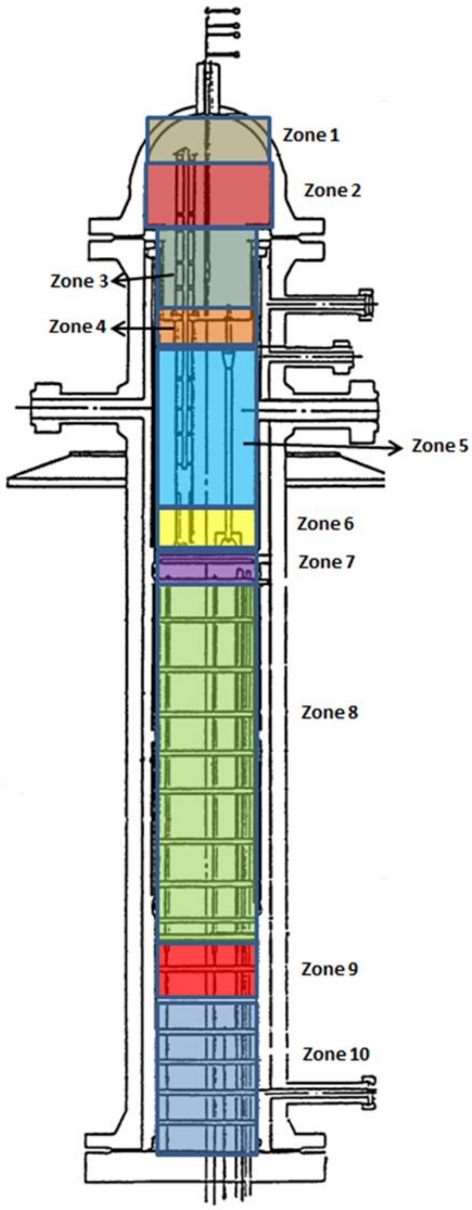

Figure 2. Axial modelling

Radial discretisation

This second discretisation permits to divide the section of the pressure vessel into four meshes and three zones. This choice is strictly related to the core geometry. Starting from the outside of the pressure vessel, the first external radial mesh represents the downcomer channel (the white crown in Figure 3). At the same time the core is characterised by three power intensity regions as described in the report [1]. This is why three radial meshes are chosen. At the same time the core is radially characterised by two porosity values and so two zones are finally sufficient. Remember that the porosity depends on different rods distribution and dimension. This is why a first radial discretization is performed starting from radius values (so we have three meshes) and a second one based on the porosity (two zones).

Meshes in the core are defined starting from the following (see Figure 3) radii:

- R1 = 0.0 mm
- R2 = 88.2 mm
- R3 = 176.4 mm
- R4 = 257.0 mm

On the other side zone depends on the porosity. Let us so define the two regions for the core: the first one from R3 to R4 corresponding to the blue region (Figure 3) and the second one from R1 to R3, corresponding to the red and the green area. Figure 3 shows the core radial discretisation.

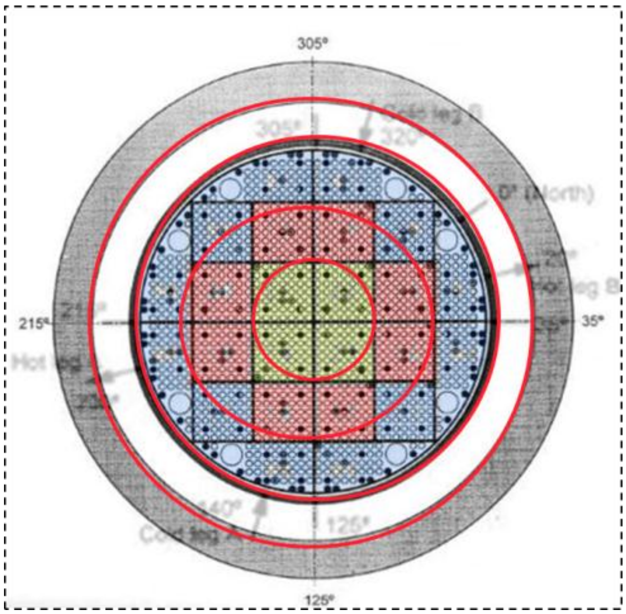

Figure 3. Radial core modelling

Azimuthal discretisation

Since the presence of two cold and two hot legs, it is suggested to consider six azimuthal zones of 60° each.

Concerning the walls modelling, they are defined starting from the experimental system geometry:

- External walls: the PV external walls made of inox316.
- Core: rod bundles electrically heated.
- Lower plenum: rod bundles that do not produce power (no heat production) but absorb coolant thermal energy.
- Core barrel: since heat exchange between downcomer channel and the core is observed during different transients, an exchanger module is chosen to represent the core barrel. The same approach was followed for the 0D-1D modelling.

CCFL modelling

Now, in order to improve the calculation in counter current flow condition and analyse its limitation, CCFL CATHARE operator has been used in the hot legs, at the vertical node after the bend.
The correlation used is Wallis type (ECCFL=0):

$J_G^{*0.5}$+m. $J_L^{*0.5} = C$, with m = 0.60, C = 0.61 and S_{ratio}=1

In the previous 1D-0D input deck a second CCFL condition was imposed at the top of the core. In the case of a 3D module the counter current flow phenomenon is taken intrinsically into account. The presence of different meshes at the core exit will simulate the automatic up flow and down flow coolant motion.

Figure 4 shows the modelling of ROSA pressure vessel using the GUITHARE visual tool.

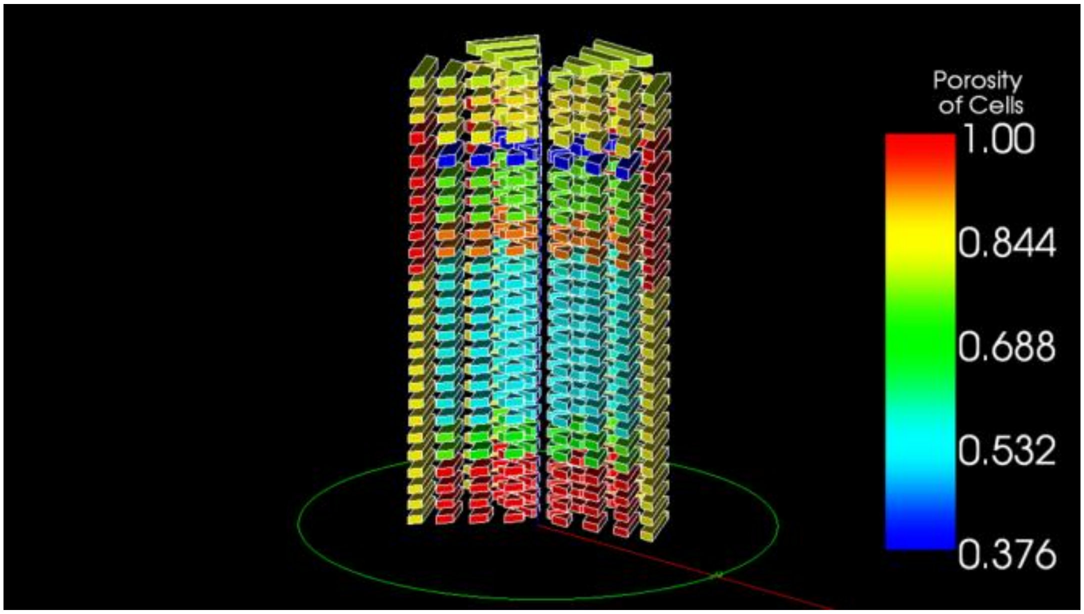

Figure 4. ROSA modelling visualization

III – TEST SCENARIO

A first validation of the 3D modelling is realised for the test 1, an intermediate (17%) hot leg break.
Firstly the system is maintained at the initial conditions and the pressurizer is isolated from the primary cooling system by closure of a valve located on the surge line. The experiment starts once all nominal conditions are reached [2]. As the electrical core power is limited to 14 % of the scaled nominal value (10 MW), the primary flowrate is also limited to this value (14 % of the scaled nominal flowrate) in order to reproduce the primary fluid temperature distribution. The accumulator of loop A represents 3 reactor scaled accumulators and the accumulator of loop B represents 1 reactor scaled accumulator. The same distribution is done for the low pressure safety injection. Note that this repartition was chosen although the loop A and B represents two reactor loops and that break is located on the hot leg of the loop B. The break is assumed on the surge line of the pressurizer (17 % of the hot leg flow area) and is experimentally simulated with a 41 mm diameter and 512 mm long nozzle, upward vertically oriented. The test transient starts 70 s after, by the opening of the break valve (t = 0).
The SCRAM signal is obtained at 1 s. The other actions are regrouped in the Table II. Total failure of both high pressure injection system and of the auxiliary feedwater is assumed. The accumulators and low pressure injection flow rate is 3:1 to cold legs of intact and broken loops, respectively. Non-condensable gas inflow from ACC tank may take place. This size of break causes a fast transient of phenomena. The detailed experimental conditions for this test and the experimental results are provided by the experimental report [2].

Table II: ROSA test scenario

Events	**LSTF**	**CATHARE**
Pressurizer isolation by valve closure	-63 s	< 0
Break valve open, increase of pump speed	0	0
SCRAM signal, closure of the SG steam stop valve	1 s	1 s
Closure of SG MSIVs	0	0
Initiation of pump coastdown	5 s	5 s
Initiation of decrease of liquid level in SG U-tubes	~10 s	~10 s
Core power decrease	20 s	20 s
Primary pressure below the secondary one	~55 s	~55 s
Accumulator (A & B) injection initiation	~155 s	~155s
Liquid accumulator B injection stops	~240 s	~300 s
Liquid accumulator A injection stops	~250 s	~280 s
LP safety injection initiation	505 s	~250 s
End of the comparison	600 s	600 s

IV – VALIDATION OF THE 3D

This paragraph presents the comparison between CATHARE computations (3D calculations) and experimental results. A further comparison with the previous results obtained using a 1D-0D model (1D-calculations) for the pressure vessel is also proposed. Some interesting results are presented from Figure 5 to Figure 11. The black, the blue (with circle) and the red (with rhombus) lines represent respectively experimental, 3D and the 1D results.

Figure 5 shows the total power produced by electrical heaters (rod bundles). It should represent the shutdown in a real PWR reactor. Starting from a value of about 10.8 MW, power shuts at about 2 MW at 300 s.

The pressure trend taken on the bottom of the pressure vessel is presented in Figure 6. It is clear that pressure values simulated by CATHARE code are in good agreement with experimental results. A first flashing and the corresponding pressure drop is well simulated by the code.

Figure 7, Figure 8, and Figure 9 show DP values measured in the upper plenum, in the core and in the downcomer. Figure 7 shows a very good agreement with the experimental results: the 3D calculation considers a complete voiding of this volume as observed during the experiment. A good correspondence of the DP in the core region is also observed.

Experimental temperatures are measured by thermocouples located inside the Inconel cladding, at 1 mm depth. They are here compared with the calculated ones, which correspond to the cladding surface values. Figure 10 shows the comparison of the maximum value of the cladding temperature in the core.

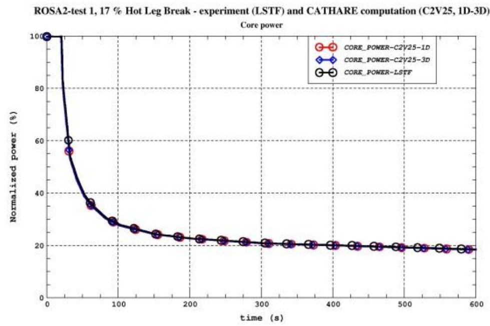

Figure 5. Core power

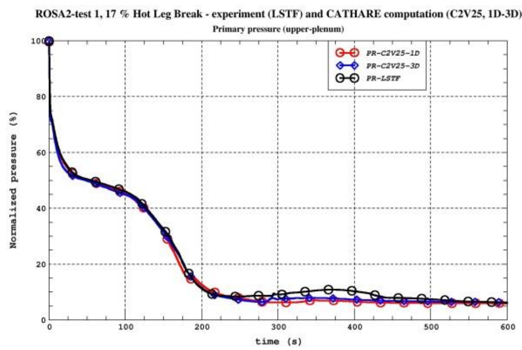

Figure 6. Pressure trend

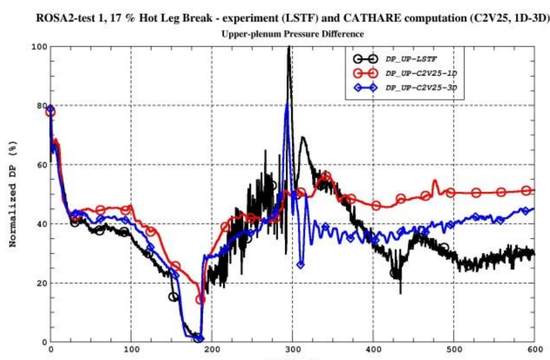

Figure 7. Upper plenum pressure difference

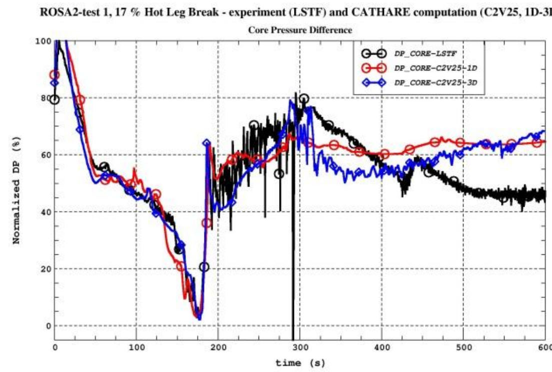

Figure 8. Core pressure difference

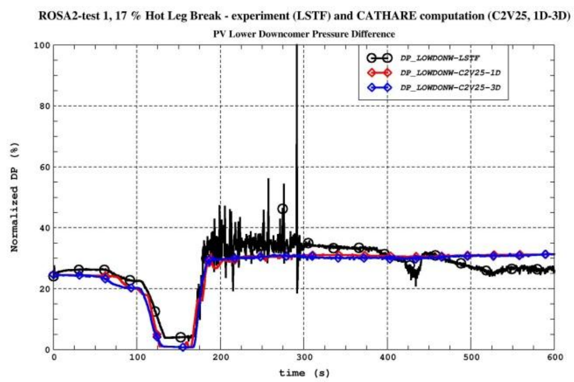

Figure 9. Lower downcomer pressure difference

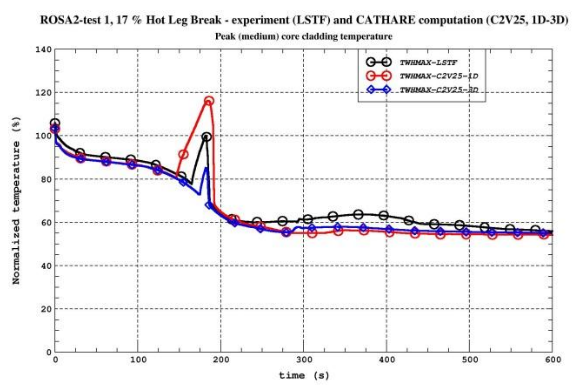

Figure 10. Temperature in the core rod

Figure 11 shows the DP measured in the SG of the loop A. Calculated points are taken at the same elevations than the experimental ones. In particular for the DP between the bottom and the top of the SG U-tube, the 6 measurements, made on 6 different U-tubes with 3 different heights, are compared with the unique value obtained with the single 1D component representation. The 3D calculations are in a good agreement with the experimental results (concerning the liquid levels and pressure trends), having a better behaviour in comparison with the 1D computation. Concerning the liquid fallback, important 3D effects are observed during the core uncovery, both in the experiment and in the3D computation. In the 1D the overall liquid fallback was underestimated via the CCFL model and the core temperature was higher that experimental one; differently in the 3D. This point will be better analysed in the future.

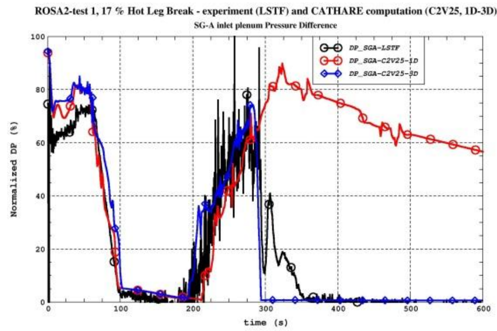

Figure 11. Pressure difference in the SG-A

V - 3D SPECIFICATIONS

Figure 12 and Figure 13 show liquid and gas flowrate calculated by CATHARE code versus time. Curves correspond to the different angular sectors (from 1 to 6), in the second crown (the middle one), at about 5 m from the bottom of the PV. The 3D behaviour is here well observed: at about 160 s the liquid flowrate may be zero, positive and negative for the different angular sectors. The same for the gas flow rate. Moreover some kind of counter current phenomena (at about 160 s for instance) may be observed starting from this 3D analysis. At this time liquid and gas flowrate are characterised by opposite directions. The same behaviour is observed just before 300 s.

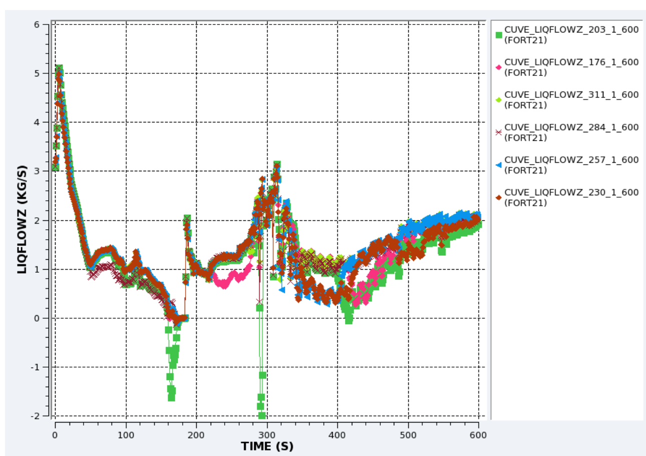

Figure 12. Liquid flowrate vs time. Curves correspond to the different sectors (1 to 6) in the second crown (the middle one) at about 5 m from the bottom of the PV

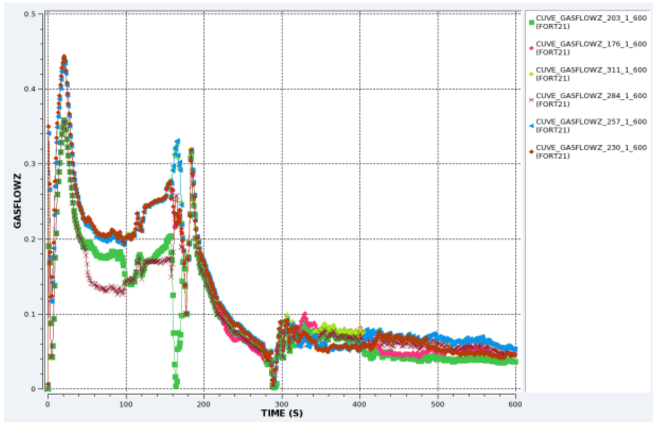

Figure 13. Gas flowrate vs time. Curves correspond to the different sectors (1 to 6) in the second crown (the middle one) at about 5 m from the bottom of the PV

Figure 14 and Figure 15 show the liquid and gas flowrate at the core exit, just below the end box, at 154 s. An important liquid flowrate goes down, in particular in the external crown (till -3 kg/s). At the same time a counter current is observed in this region since the positive direction of gas flowrate practically everywhere at this elevation. Note that if the positive gas flowrate rises, it carries the liquid mass and the descent liquid flowrate decreases. Important 3D effects are here observed.

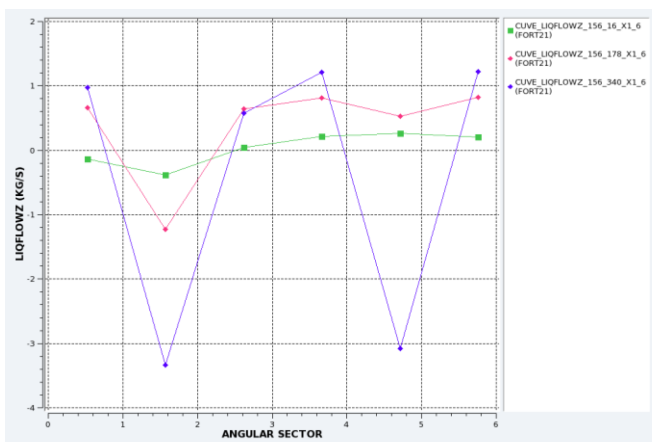

Figure 14. Liquid flowrate at 154 s vs angular sectors. Curves correspond to different crown (internal-green, medium-red and external-blue)

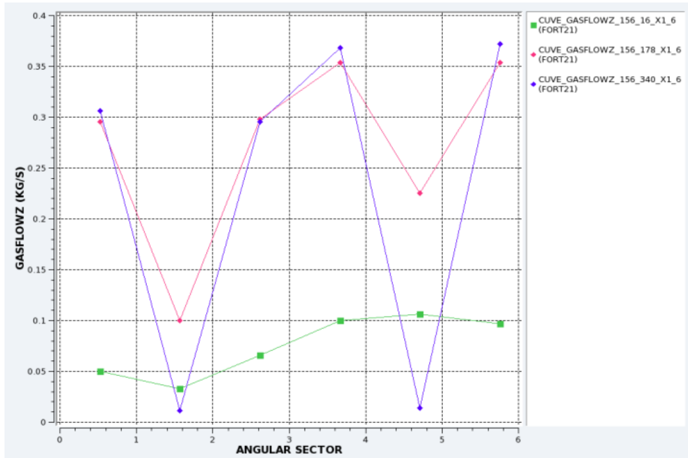

Figure 15. Gas flowrate at 154 s vs angular sectors. Curves correspond to different crown (internal-green, medium-red and external-blue)

Figure 16 shows the void fraction calculated by CATHARE from the bottom to the top of the pressure vessel in the external crown (third radius). Time is between 156 sand 186 s. At about 6 m we have the end box, between 6 m and 8 m we have the upper plenum. The core support plate is at about 9 m. The upper head is between 9 m and 11 m. Figure 16 shows that at about 180 s the core region is completely voided (void fraction = 1) and the upper plenum starts to be completely voided before 170 s. This behaviour is in agreement with Figure 9 since the pressure difference is practically zero at this time.

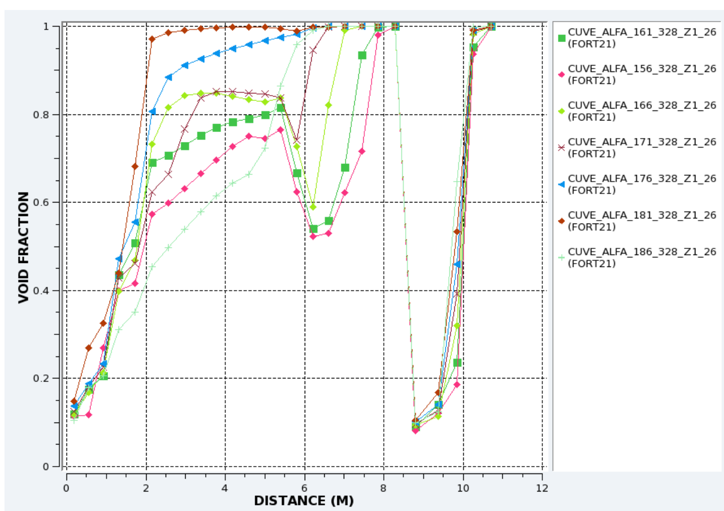

Figure 16. Void fraction vs PV elevation. Curves corresponds to different times (from 156 s to 186 s) measured in the external crown and sector 1. These values are taken in the end box level.

A useful visualisation of the void fraction evolution is presented in Figure 17 . At about 154 s (just at the accumulator injection initiation) the downcomer region is practically voided. It corresponds to the experimental evidence presented in Figure 9. At about 180 s, after the loop seal clearing caused by the accumulator injection, the core zone is practically emptied of liquid corresponding to Figure 9 and the downcomer zone largely refilled.

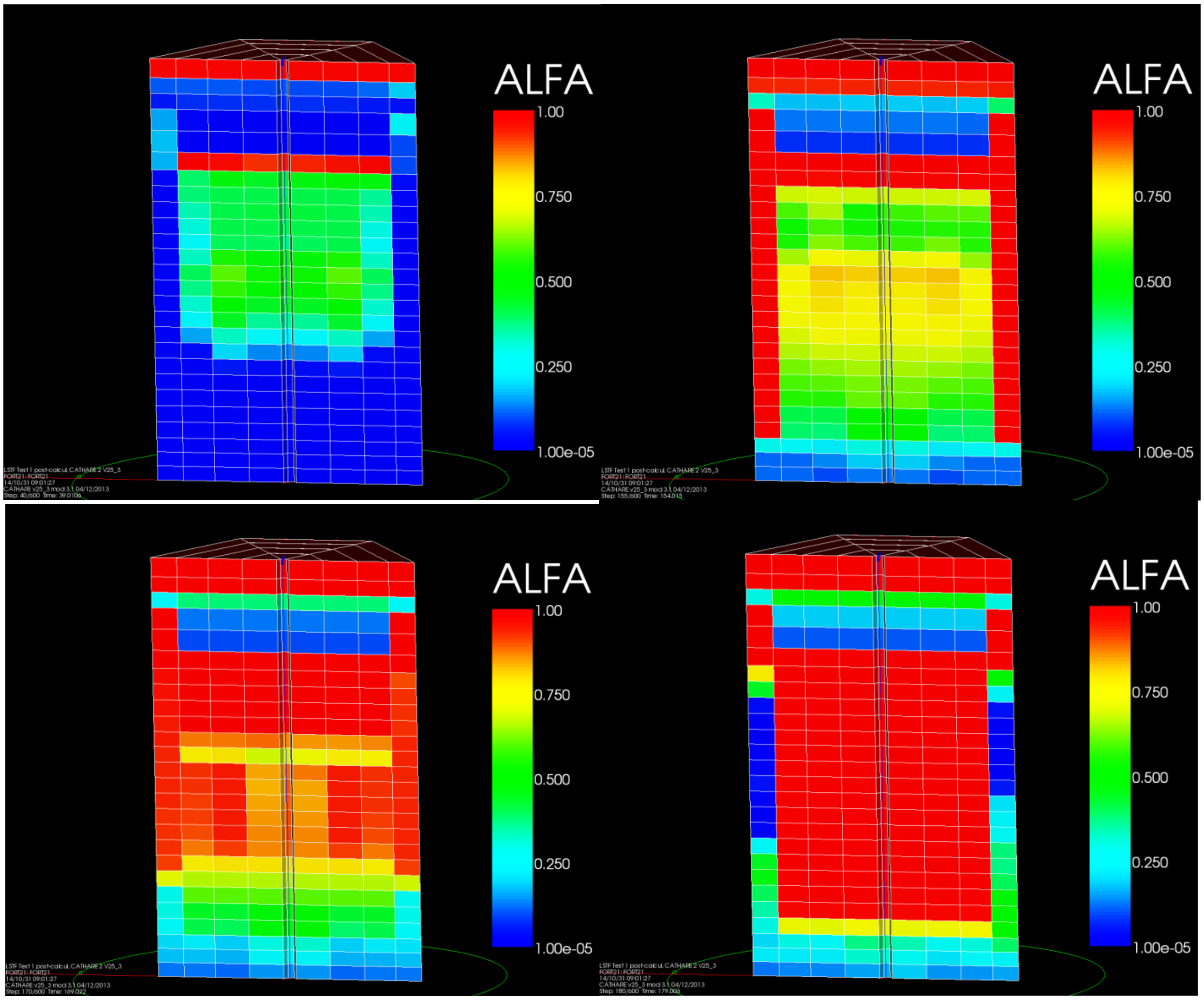

Figure 17. Void fraction vs time (39 s - 154 s - 169 s – 179 s)

Figure 18 shows the cladding temperature distribution versus time measured at about 5 m from the bottom of the pressure vessel. This value is plotted for all high power heater rods. Heater rods present in the second crown are hotter than that present in the external region. The temperature peak difference may be 20 °C. Also in this case the 3D effects are well observed.

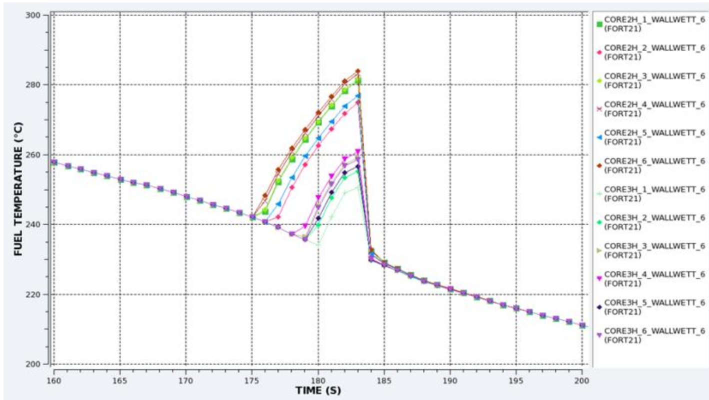

Figure 18. Fuel temperature vs time. Curves correspond to the hotter fuel rods values at 5 m from the bottom of the PV

VI – CONCLUSIONS

An important work aimed to validate the 3D module of CATHARE code applied to the ROSA installation is here presented. A first comparison of the 3D CATHARE calculation to the measurements and to the 1D calculation for the entire transient corresponding to ROSA2 test n°1 is performed. This comparison shows a good agreement of the 3D calculation with the experiment till the second half of the accumulator injection (roughly 250 s).

A real improvement related to the 1D computation is also observed in particular concerning the fluid distribution between the core and the upper-plenum, the overall liquid fall back, the core heat-up (a good heat-up trend) and the primary depressurization during the core uncovery.

A detailed analysis of the 3D phenomena foreseen by the computation is also presented. Some rather strong 3D effects are predicted during the core level depletion; in particular the liquid flowrates show different directions according the location in the core. Due to the lack of real 3D measurements, these 3D phenomena may be only globally validated, mainly through DP measurements.

This first validation will be followed by the analysis of two other intermediate break tests (n°2 and n°7) of OCDE/AEN ROSA2 project. The final purpose of this work is the validation of the 3D model for different scenarii and different 3D phenomena. This action will permit to obtain a more solid code, able to better represent the entire system and to predict its global behaviour.

ACKNOWLEDGMENTS

The present work contains findings that are produced within the OECD/NEA ROSA-2 Project. The authors are grateful to the Management Board of this project for its consent to this publication.

REFERENCES

[1] The ROSA V Group, 'ROSA-V Large Scale Test Facility (LSTF) – System description for the third and fourth simulated fuel assembly', JAERI Tech/2003-037, March 2003,.

[2] The ROSA V Group, 'Final Data Report of ROSA-2/LSTF Test 1, (Hot Leg Intermediate Break LOCA IB-HL-01)', September 2011.